

# Effective three-body interactions in the $\alpha$ -cluster model for the $^{12}\text{C}$ nucleus

S. I. Fedotov, O. I. Kartavtsev, and A. V. Malykh

*Joint Institute for Nuclear Research, Dubna, 141980, Russia*

## Abstract

Properties of the lowest  $0^+$  states of  $^{12}\text{C}$  are calculated to study the role of three-body interactions in the  $\alpha$ -cluster model. An additional short-range part of the local three-body potential is introduced to incorporate the effects beyond the  $\alpha$ -cluster model. There is enough freedom in this potential to reproduce the experimental values of the ground-state and excited-state energies and the ground-state root-mean-square radius. The calculations reveal two principal choices of the two-body and three-body potentials. Firstly, one can adjust the potentials to obtain the width of the excited  $0_2^+$  state and the monopole  $0_2^+ \rightarrow 0_1^+$  transition matrix element in good agreement with the experimental data. In this case, the three-body potential has strong short-range attraction supporting a narrow resonance above the  $0_2^+$  state, the excited-state wave function contains a significant short-range component, and the excited-state root-mean-square radius is comparable to that of the ground state. Next, rejecting the solutions with an additional narrow resonance, one finds that the excited-state width and the monopole transition matrix element are insensitive to the choice of the potentials and both values exceed the experimental ones.

PACS numbers: 21.45.+v, 21.60.Gx, 23.60.+e, 24.30.Gd

## I. INTRODUCTION

As the  $\alpha$ -particle is the most tightly bound nucleus, a variety of the low-energy nuclear properties can be successfully described within the framework of the  $\alpha$ -cluster model. The effective two-body and, for more than two  $\alpha$ -particles, at least three-body potentials must be determined as an input for the model. The three-body calculations allow one to reduce ambiguity in the two-body potential which could not be determined merely from the two-body data. In this respect, the basic problem is to check the model for the system of three  $\alpha$ -particles, thus, the effective potentials should be chosen by fitting the main characteristics of the  $^{12}\text{C}$  nucleus to the experimental values.

In spite of significant simplifications provided by the  $\alpha$ -cluster model, there are complicated problems inherent in the processes with few charged particles in the initial or final state. For the problems of this kind the main difficulty stems from the necessity to describe the continuum wave function and even qualitative understanding of the reaction mechanism is crucial. The formation of the  $^{12}\text{C}$  nucleus in the triple- $\alpha$  low-energy collisions, which plays a key role in stellar nucleosynthesis [1, 2], is a well-known example. More examples are double-proton radioactivity, which has been a subject of thorough experimental and theoretical investigations during the last years (for details see the recent reviews [3, 4]) and decay of the long-lived  $^{12}\text{C}(1^+)$  state [5]. Note also a description of multi-cluster decay of atomic nuclei by using the quasi-classical approach to Coulomb-correlated penetration through a multidimensional potential barrier [6].

In the triple- $\alpha$  reaction both the low-energy  $\alpha$ - $\alpha$  resonance (the ground state of  $^8\text{Be}$ ) and the near-threshold three-body resonance ( $^{12}\text{C}(0_2^+)$  state) play an important role. These resonances are predicted in Ref. [2] as unique possibility for helium burning that provides the only explanation for observable abundance of elements in the universe. Due to these resonances, the triple- $\alpha$  reaction in stars goes through the sequential reaction  $3\alpha \rightarrow ^8\text{Be} + \alpha \rightarrow ^{12}\text{C}(0_2^+) \rightarrow ^{12}\text{C} + \gamma$ . The predicted  $^{12}\text{C}(0_2^+)$  state, starting with the observation [7, 8], was thoroughly studied later on, in particular, the decay mechanism was investigated in Ref. [9]. The corresponding theoretical problem is the microscopic calculation of the resonance width extremely small on the nuclear scale and the  $0_2^+ \rightarrow 0_1^+$  monopole transition matrix element (MTME).

Among other interesting problems connected with description of  $\alpha$ -cluster nuclei, one

should mention the nonresonance reaction  $3\alpha \rightarrow {}^{12}\text{C}$ , which is responsible for helium burning at ultra-low temperatures and high densities as in accretion on white dwarfs and neutron stars [10]. Whereas a number of model calculations of the nonresonance reaction are available [11, 12, 13, 14], a consistent three-body description is needed to avoid a possible error of a few orders of magnitude in the calculated reaction rate. Note also that recently the  $\alpha$ -cluster states in nuclei have attracted attention in connection with the problem of  $\alpha$ -particle condensation (see, e. g., Ref. [15] and references therein).

A focus of the present paper is to shed light, using the technique of Ref. [16], on the role of the three-body interactions in description of the lowest  $0^+$  states of  ${}^{12}\text{C}$ . The main question to be answered is to what extent the  $\alpha$ -cluster model is able to reproduce the experimental energies and sizes of the nuclear states. The next one, more challenging problem, is to describe the fine characteristics, such as the width of the near-threshold  $0_2^+$  state and  $0_2^+ \rightarrow 0_1^+$  MTME, which are sensitive to the choice of the potentials. In realistic calculations, the finite size of the  $\alpha$ -particle implies crucial importance of the effective three-body interactions for reliable description within the framework of the  $\alpha$ -cluster model [16, 17, 18]. Furthermore, the effective three-body interactions could be used to take into account the non- $\alpha$ -cluster structure of the nucleus at short distances in addition to the effect of  $\alpha$ -particle distortions at large distances. Clearly, the choice of the effective two-body and three-body potentials must be governed by the results of the three-body calculations aimed at optimal description of the  ${}^{12}\text{C}$  characteristics.

## II. THEORETICAL BACKGROUND

The present paper is aimed to chose, by means of microscopic three-body calculation of the ground and first excited  $0^+$  states of  ${}^{12}\text{C}$ , the effective three-body and two-body potentials of the  $\alpha$ -cluster model. It is assumed that all the effects connected with both the internal structure of  $\alpha$ -particles and the identity of nucleons are incorporated in the effective potentials. The two-body input is defined by the local  $\alpha$ - $\alpha$  potential that reproduces the experimental energy and width of the near-threshold  $\alpha$ - $\alpha$  resonance (ground state of  ${}^8\text{Be}$ ). More precisely, with the  ${}^8\text{Be}$  energy fixed and its width varying within the experimental uncertainty, a set of two-body potentials is constructed by modification of the Ali-Bodmer s-wave potential [19]. One uses a simple, and suitable for calculation, functional form of

the three-body potential, which depends only on the collective variable, viz, the hyper-radius. A sum of two Gaussian terms is used, which makes it possible to take into account both the effect of  $\alpha$ -particle distortions at large distances and the short-range non- $\alpha$ -cluster effects. Calculation of the resonance width and the MTME makes sense only if, not only the ground-state energy but also the resonance position and the root-mean-square (rms) radius of the ground state are fixed at the experimental values. These requirements are satisfied by adjusting the parameters of the three-body potential.

The technical details and the numerical procedure are basically the same as in the previous paper [16], therefore, only a sketch of the calculational method will be given below. The method is based on the expansion of the total wave function in terms of the eigenfunctions on a hypersphere [20]. The eigenvalue problem on a hypersphere is numerically solved by using the variational method.

The units  $\hbar = m = e = 1$  are used throughout the paper unless other is specified. The scaled Jacobi coordinates are defined as  $\mathbf{x}_i = \mathbf{r}_j - \mathbf{r}_k$ ,  $\mathbf{y}_i = (2\mathbf{r}_i - \mathbf{r}_j - \mathbf{r}_k)/\sqrt{3}$ , where  $\mathbf{r}_i$  is the position vector of the  $i$ th particle. The hyper-spherical variables  $\rho$ ,  $\alpha_i$ , and  $\theta_i$ , are defined via the Jacobi coordinates by the relations  $x_i = \rho \cos \frac{\alpha_i}{2}$ ,  $y_i = \rho \sin \frac{\alpha_i}{2}$ , and  $\cos \theta_i = \frac{(\mathbf{x}_i \mathbf{y}_i)}{x_i y_i}$ .

The Schrödinger equation for three  $\alpha$ -particles is

$$\left( -\Delta_{\mathbf{x}} - \Delta_{\mathbf{y}} + \sum_{j=1}^3 V(x_j) + V_3(\rho) - E \right) \Psi = 0, \quad (1)$$

where the total interaction contains the pair-wise potentials  $V(x_i)$  and the three-body potential  $V_3(\rho)$ . The two-body potential is a sum  $V(x) = V_s(x) + V_c(x)$ , where

$$V_s(x) = V_r e^{-\mu_r^2 x^2} - V_a e^{-\mu_a^2 x^2} \quad (2)$$

and  $V_c(x) = \frac{4}{x}$ . The three-body potential is taken as an obvious extension of the potential used in Refs. [16, 17, 18],

$$V_3(\rho) = V_0 e^{-(\rho/b_0)^2} + V_1 e^{-(\rho/b_1)^2}. \quad (3)$$

With the expansion of the total wave function

$$\Psi = \rho^{-5/2} \sum_n f_n(\rho) \Phi_n(\alpha, \theta, \rho) \quad (4)$$

in a series of the normalized eigenfunctions  $\Phi_n$  satisfying the equation on the

$$\left[ \frac{\partial^2}{\partial \alpha^2} + 2 \cot \alpha \frac{\partial}{\partial \alpha} + \frac{1}{\sin^2 \alpha} \left( \frac{\partial^2}{\partial \theta^2} + \cot \theta \frac{\partial}{\partial \theta} \right) - \right.$$

(5)

$$\frac{\rho^2}{4} \sum_{j=1}^3 V \left( \rho \cos \frac{\alpha_j}{2} \right) + \lambda_n(\rho) \Big] \Phi_n(\alpha, \theta, \rho) = 0 ,$$

the Schrödinger equation (1) is routinely transformed to the system of hyper-radial equations (HRE)

$$\left[ \frac{\partial^2}{\partial \rho^2} - \frac{1}{\rho^2} \left( 4\lambda_n(\rho) + \frac{15}{4} \right) - V_3(\rho) + E \right] f_n(\rho) +$$

(6)

$$\sum_m \left( Q_{nm}(\rho) \frac{\partial}{\partial \rho} + \frac{\partial}{\partial \rho} Q_{nm}(\rho) - P_{nm}(\rho) \right) f_m(\rho) = 0 ,$$

$$Q_{nm}(\rho) = \left\langle \Phi_n \left| \frac{\partial \Phi_m}{\partial \rho} \right. \right\rangle , P_{nm}(\rho) = \left\langle \frac{\partial \Phi_n}{\partial \rho} \left| \frac{\partial \Phi_m}{\partial \rho} \right. \right\rangle ,$$

(7)

where  $\langle \cdot | \cdot \rangle$  stands for integration on the hyper-sphere.

The functions  $\lambda_n(\rho)$ ,  $Q_{nm}(\rho)$ , and  $P_{nm}(\rho)$  are calculated by using the variational solutions of the eigenvalue problem (5). In view of the symmetry of  $\Phi_n(\alpha, \theta, \rho)$ , which follows from the identity of  $\alpha$ -particles, the variational trial functions are chosen to be symmetric under any permutation of particles. Few types of trial functions are used, which provides flexibility of the variational basis needed to describe an essentially different structure of the wave function at different values of  $\rho$ , in particular, the two- and three-cluster configurations in the asymptotic region. Thus, the variational basis contains a set of the symmetric hyper-spherical harmonics which are eigenfunctions of the differential operator in Eq. (5). Furthermore, to describe the two-cluster configuration, symmetrized combinations of the  $\rho$ -dependent two-body functions  $\phi_i(x)$  are included in the basis. As in Ref. [16], a set of  $\phi_i(x)$  includes Gaussian functions  $\phi_i(x) = \exp(-\beta_i x^2)$ , which allows the two-cluster wave function to be described within the range of the nuclear potential  $V_s(r)$ , and the function  $\phi(x) = x^{1/4} \exp(-4\sqrt{x}(1+ax))$  to describe the two-cluster wave function in the sub-barrier region.

Solutions of the eigenvalue problem (at  $E < 0$ ) and the  $\alpha + {}^8\text{Be}$  scattering problem (at  $E > 0$ ) for HRE (6) provide the properties of the ground  $0_1^+$  state and the excited  $0_2^+$  resonance state, respectively. The resonance position  $E_r$  and width  $\Gamma$  are determined by fitting the scattering phase shift  $\delta_E$  to the Wigner dependence on energy

$$\cot(\delta_E - \delta_{bg}) = \frac{2}{\Gamma}(E_r - E) ,$$

(8)

where the background phase shift  $\delta_{bg}$  is of no interest for the present calculation. It is suitable to treat the ultra-narrow  $0_2^+$  resonance state on equal footing with the ground state. Therefore, its wave function, defined as the scattering solution at the resonance energy  $E_r$ , is normalized on the finite interval  $0 \leq \rho \leq \rho_t$ , where  $\rho_t$  is the turning point of the first-channel hyper-radius potential  $U_1(\rho) = \frac{1}{\rho^2} \left( 4\lambda_1(\rho) + \frac{15}{4} \right) + V_3(\rho) + P_{11}(\rho)$ . Thus, the rms radii  $R^{(i)}$  of the ground ( $i = 1$ ) and excited ( $i = 2$ ) states and MTME  $M_{12}$  are defined by the expressions

$$R^{(i)} = \sqrt{R_\alpha^2 + \frac{1}{6}\bar{\rho}_i^2}, \quad \bar{\rho}_i^2 = \sum_n \int_0^\infty |f_n^{(i)}(\rho)|^2 \rho^2 d\rho, \quad (9)$$

where  $R_\alpha = 1.47$  fm is the rms radius of the  $\alpha$ -particle, and

$$M_{12} = \sum_n \int_0^{\rho_t} f_n^{(2)}(\rho) f_n^{(1)}(\rho) \rho^2 d\rho. \quad (10)$$

### III. RESULTS

Calculations have been performed with a family of the two-body  $\alpha$ - $\alpha$  potentials  $V_s$  (2), which are obtained by modification of potential (a) from Ref. [19]. With the ranges of the repulsive and attractive parts fixed at the values  $\mu_r^{-1} = 1.53 fm$  and  $\mu_a^{-1} = 2.85 fm$ , the parameters  $V_r$  and  $V_a$  were chosen to reproduce the experimental energy  $E_{2\alpha} = 91.89$  keV [21] of the  $\alpha$ - $\alpha$  resonance (ground state of  $^8\text{Be}$ ) and to vary its width within the experimental uncertainty  $\gamma = 6.8 \pm 1.7$  eV [21]. As the width  $\gamma$  unambiguously determines the parameters of the two-body potential, in the following the potential will be marked by  $\gamma$ . A partial set of the parameters  $V_r$  and  $V_a$  and the widths  $\gamma$  is presented in Table I.

The three-channel system of HREs (6) is solved to calculate the ground- and excited-state energies  $E_{gs}$  and  $E_r$ , the rms radii  $R^{(i)}$ , the excited-state width  $\Gamma$ , and the monopole transition matrix element  $M_{12}$ . Convergence in a number of HRE is sufficiently fast and solution of three HRE allows the resonance width to be determined with an accuracy not worse than 1 eV. Generally, the parameters of the numerical procedure and an accuracy of the calculated  $E_{gs}$ ,  $E_r$ ,  $\Gamma$ ,  $R^{(i)}$ , and  $M_{12}$  were the same as in Ref. [16]. Using the numerical procedure of determination of  $E_{gs}$ ,  $E_r$ , and  $R^{(1)}$ , the parameters of the three-body potential for each two-body potential were determined by solving the nonlinear inverse problem of fixing the ground- and excited-state energies and the excited-state rms radius at the experimental values  $E_{gs} = -7.2747$  MeV,  $E_r = 0.3795$  MeV [22], and  $R_{exp}^{(1)} = 2.48 \pm 0.22$  fm [23, 24].

TABLE I: Parameters of the  $\alpha$ - $\alpha$  potential  $V_s$  (2) providing the  $\alpha$ - $\alpha$  resonance widths  $\gamma$ .

$\gamma(\text{eV})$	$V_r(\text{MeV})$	$V_a(\text{MeV})$
5.69	35.024	19.492
6.20	52.772	22.344
6.37	60.051	23.359
6.40	61.220	23.516
6.50	66.028	24.141
6.60	71.057	24.766
6.80	82.563	26.1

At the first stage of the calculations only the one-term potential ( $V_1 = 0$ ) was studied for better understanding of the dependence on the three-body potential  $V_3(\rho)$  (3). For this two-parameter potential, only  $E_{gs}$  and  $E_r$  are fixed at the experimental values to determine  $V_0$  and  $b_0$ . The calculation gives two types of solutions, that is, two families of one-term three-body potentials, whose parameters  $V_0$  and  $b_0$  are presented in Table II. For one type of solutions, three-body potentials are rather extended with the range about  $b_0 = 4.5$  fm and strength  $|V_0| < 40$  MeV. The ground-state rms radius is in the range  $2.2 \text{ fm} < R^{(1)} < 2.8 \text{ fm}$ , which includes the experimental value, whereas  $\Gamma$  and  $M_{12}$  significantly exceed the experimental values  $\Gamma = 8.5 \pm 1.0 \text{ eV}$  and  $M_{12} = 5.48 \pm 0.22 \text{ fm}^2$  [22]. For another type of solutions,  $b_0$  is about twice as small and  $|V_0|$  exceeds 80 MeV. The ground-state rms radius is lower than  $R_{exp}^{(1)}$ , nevertheless,  $\Gamma$  and  $M_{12}$  are in better agreement with experiment than in the previous case. As the ground-state size  $R^{(1)}$  cannot be fixed at the experimental value by using the one-term three-body potential, it is not surprising that finer properties  $\Gamma$  and  $M_{12}$  vary in a wide range with variations of the two-body potential.

The results for the one-term potential ( $V_1 = 0$ ) clearly show lack of simultaneous description for the ground-state size  $R^{(1)}$  and the excited-state characteristics  $\Gamma$  and  $M_{12}$ . As far as it does not seem reasonable to improve agreement between calculation and experiment for the very fine properties  $\Gamma$  and  $M_{12}$  at the expense of the ground-state rms radius, one concludes that the one-term three-body potential is too simple to describe the real nucleus. One can readily propose to contaminate both the short-range and the long-range term in the three-body potential to obtain compromising description of the ground-state

TABLE II: Two families of solutions with the one-term three-body potential ( $V_1 = 0$ ) for a number of two-body potentials marked by the widths  $\gamma$  (eV) of the  $\alpha$ - $\alpha$  resonance. Shown are the parameters  $b_0$  (fm) and  $V_0$  (MeV), rms radii  $R^{(i)}$  (fm), width of the excited state  $\Gamma$  (eV), and monopole transition matrix element  $M_{12}$  (fm<sup>2</sup>).

$\gamma$	$b_0$	$V_0$	$\Gamma$	$R^{(1)}$	$R^{(2)}$	$M_{12}$	$b_0$	$V_0$	$\Gamma$	$R^{(1)}$	$R^{(2)}$	$M_{12}$
5.69	4.5001	-18.600	13.0	2.35	3.7	8.59	2.2310	-89.941	8.2	2.02	3.4	6.46
6.20	4.6006	-20.824	15.9	2.45	3.8	8.87	2.3314	-113.28	9.7	2.09	3.5	6.90
6.37	4.6247	-21.643	16.9	2.48	3.9	8.93	2.3472	-125.05	10.2	2.12	3.5	7.01
6.40	4.6455	-21.640	17.2	2.48	3.9	8.97	2.3464	-127.48	10.4	2.12	3.5	7.03
6.50	4.6379	-22.297	17.6	2.50	3.9	8.97	2.3547	-135.38	10.7	2.13	3.5	7.09
6.60	4.6455	-22.838	18.1	2.51	3.9	8.99	2.3584	-144.47	11.0	2.14	3.6	7.13
6.80	4.6531	-24.047	19.3	2.55	4.0	9.03	2.3611	-166.39	11.7	2.17	3.6	7.22

and excited-state characteristics.

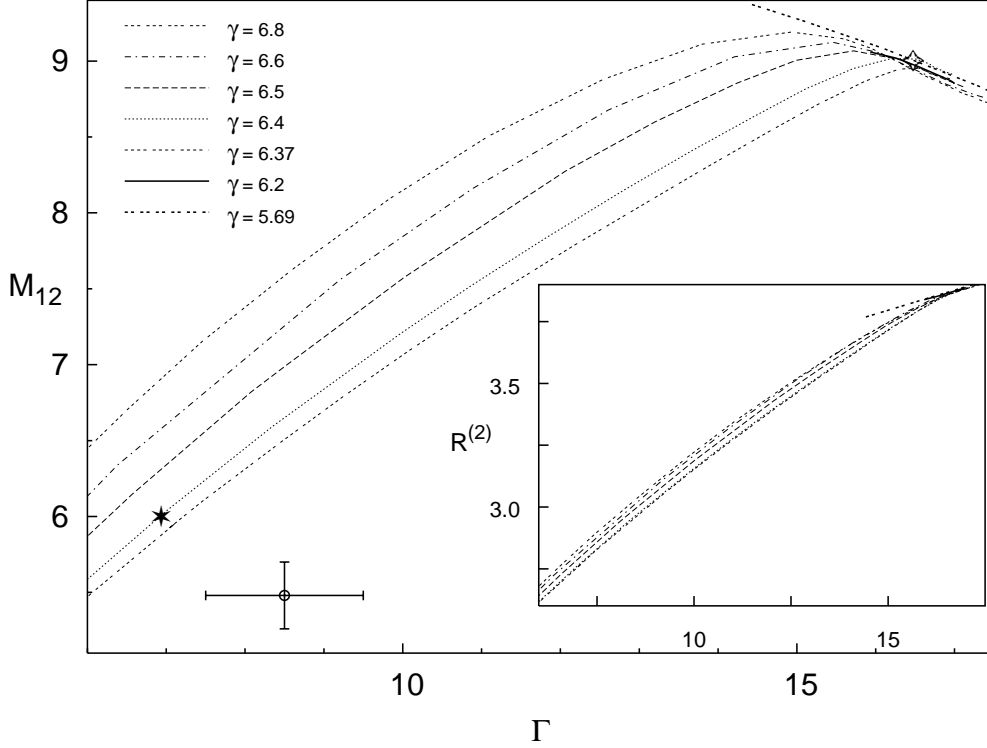
At the main route of calculations, four parameters of the three-body potential  $V_3(\rho)$  (3) are used to fix the basic properties, viz., the ground-state and excited-state energies and the ground-state rms radius at the experimental values [26]. Varying one remaining degree of freedom in the four-dimensional space of parameters  $V_{0,1}, b_{0,1}$  of the three-body potential, one obtains a one-parameter set of solutions, which is suitably represented for each two-body potential by a line in the  $\Gamma$ - $M_{12}$  plane, as shown in Fig. 1. It turns out that some of the calculated potentials, namely, those for which the parameter  $b_0 > 6$  fm, are of the form of a shallow well with a long tail. These solutions of unreasonably long range were withdrawn from the consideration and will not be presented.

Furthermore, the parameters of the long-range term in the three-body potential  $V_0 \approx 20$  MeV and  $b_0 \approx 4.5$  fm are similar to those found in the calculations with the one-term potential. Thus, the long-range tails of the four-parameter three-body potentials and one of the one-term potentials practically coincide. On the other hand, the one-term potentials of another type look like an average of the full three-body potentials at short distances. These qualitative features are seen in Fig. 2, where the first-channel hyper-radial potentials  $U_1(\rho)$  are presented.

All the solutions turn out to pass through a small common area about  $\Gamma \approx 16.5$  eV and



FIG. 1: Calculated  $M_{12}$ – $\Gamma$  relations. Each line depicts the result for the two-body potential marked by the two-body resonance width  $\gamma$ . The point with errorbars shows the experimental data. The corresponding  $R^{(2)}$ – $\Gamma$  relations are shown in the inset.



$M_{12} \approx 9 \text{ fm}^2$ , which is marked by a diamond in Fig. 1. This area is well separated from the experimental values. Correspondingly, the calculated values of the excited-state rms radius are concentrated around the value  $R^{(2)} \approx 3.9 \text{ fm}$ . This surprising insensitivity of  $\Gamma$ ,  $M_{12}$ , and  $R^{(2)}$  to the choice of the two-body and three-body potentials results from the imposed requirement to fix the ground-state rms radius at the experimental value.

The solutions could be separated in two classes, which are characterized by a sign of the short-range term in the three-body potential. The solutions of the first class ( $V_1 < 0$ ) are found for  $\gamma > 6.35 \text{ eV}$  and those of the second class ( $V_1 > 0$ ) for  $\gamma < 6.35 \text{ eV}$ . Note that this separation is correlated with the dependence of the ground-state rms radius  $R^{(1)}$  on  $\gamma$  found in the above calculations for the extended one-term potentials. If  $R^{(1)} < R_{exp}^{(1)}$ , which takes place for  $\gamma < 6.35 \text{ eV}$ , one needs to add a repulsive term ( $V_1 > 0$ ), and if  $R^{(1)} > R_{exp}^{(1)}$  (for  $\gamma > 6.35 \text{ eV}$ ), an attractive term must be added to fix  $R^{(1)}$  at the experimental value. For the second-class solutions, the larger  $\Gamma$  the smaller  $M_{12}$ , therefore, the corresponding lines never approach the experimental data. On the contrary, for the solutions of the first class

( $\gamma > 6.35$  eV), the lines in the  $\Gamma$ - $M_{12}$  plane bend downward inside the common area that provides an option to diminish simultaneously  $\Gamma$  and  $M_{12}$ .

More detailed consideration of the dependence on the two-body potential (on the parameter  $\gamma$ ) shows that the lines in the  $\Gamma$ - $M_{12}$  plane representing the solutions of the first class form a band, as seen in Fig. 1. The upper and lower borders of the band correspond to  $\gamma \approx 6.8$  eV and  $\gamma \approx 6.35$  eV, respectively. The dependence on  $\gamma$  (for  $\gamma > 6.8$  eV) becomes weak so that the lines in the  $\Gamma$ - $M_{12}$  plane are rather close to the upper border, though being inside the band. For decreasing  $\gamma$  below 6.8 eV, the lines in the  $\Gamma$ - $M_{12}$  plane shift downward until the critical value about  $\gamma \approx 6.35$  eV is reached. An abrupt transition to the second class solutions takes place at the critical value of  $\gamma$ , beyond which the lines in the  $\Gamma$ - $M_{12}$  plane always remain near the common area ( $\Gamma \approx 16.5$  eV,  $M_{12} \approx 9$  fm<sup>2</sup>). The dependence of  $R^{(2)}$  on  $\gamma$  is illustrated in the inset in Fig. 1, where it is seen that for  $\gamma > 6.35$  eV the lines lie within a narrow band in the  $\Gamma - R^{(2)}$  plane. Alternatively, for  $\gamma < 6.35$  eV, the calculated values are in a small area about  $\Gamma \approx 16.5$  eV and  $R^{(2)} \approx 3.9$  fm.

The described features are closely connected with the form of the three-body potential, in particular, the smaller  $\Gamma$ ,  $M_{12}$ , and  $R^{(2)}$  the larger the strength  $|V_1|$  of the attractive term and the smaller its range  $b_1$ . To exemplify these considerations, let us consider a typical two-body potential with  $\gamma = 6.4$  eV and a particular three-body potential, which gives  $\Gamma$  and  $M_{12}$  (marked by an asterisk in Fig. 1) sufficiently close to the experimental data. The parameters of the three-body potential,  $\Gamma$ ,  $M_{12}$ , and  $R^{(2)}$  at this point are compared in Table III with the corresponding values, which are typical of the common area (marked by a diamond). The excited-state rms radius  $R^{(2)}$ , as shown in the inset in Fig. 1, decreases with

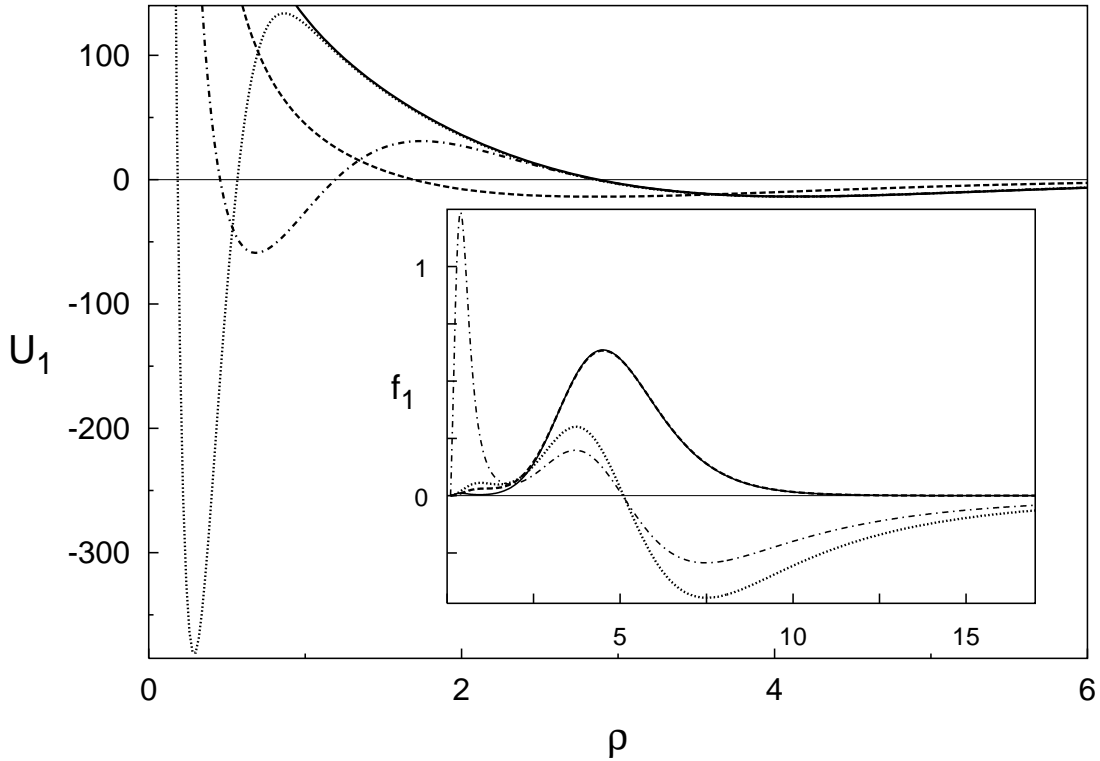
TABLE III: Parameters of the three-body potential and characteristics of the  $^{12}\text{C}(0^+)$  states. The two-body potential provides the  $\alpha$ - $\alpha$  resonance widths  $\gamma = 6.4$  eV. An asterisk and a diamond mark two solutions which are also depicted in Fig. 1.

	$V_0$ (MeV)	$b_0$ (fm)	$V_1$ (MeV)	$b_1$ (fm)	$\Gamma$ (eV)	$M_{12}$ (fm <sup>2</sup> )	$R^{(2)}$ (fm)
◇	-22.189	4.5699	-411.719	1.0155	16.5	9.01	3.86
*	-22.867	4.5109	-1710.00	0.41009	7.0	6.0	2.76

decreasing  $\Gamma$  from the typical value  $R^{(2)} \approx 3.9$  fm for solutions near the common area to  $R^{(2)} \approx 2.8$  fm for solutions near the point marked by an asterisk that only slightly exceeds

the ground-state rms radius  $R^{(1)} = 2.47$  fm. Diminishing of  $R^{(2)}$  to these small values underlines a comparatively compact structure of the excited state. Indeed, the excited-state wave functions, as shown in the inset in Fig. 2, are quite different for the solutions marked by a diamond and an asterisk. Nevertheless, the ground-state wave functions are surprisingly similar to each other.

FIG. 2: The first-channel hyper-radial potentials  $U_1(\rho)$  calculated for the two-body potential providing  $\gamma = 6.4$  eV. Dash-dotted and dotted lines depict  $U_1(\rho)$  for the three-body potentials whose parameters are marked in Table III by a diamond and an asterisk, respectively. Full and dashed lines depict  $U_1(\rho)$  for the one-term three-body potential whose parameters are given in the line 4 of Table II. The inset shows the first-channel radial functions  $f_1(\rho)$  for the potential marked by an asterisk (full and dash-dotted lines for the ground and excited states) and for the potential marked by a diamond (dashed and dotted lines for the ground and excited states).



A drastic modification of the excited-state wave function at short distances for the solution with small  $\Gamma$  and  $M_{12}$  hints that the short-range attractive well in the three-body potential is able to support a near-lying resonance state. Indeed, the calculations reveal an additional resonance, whose energy changes from about 0.5 MeV for the solutions with small

$\Gamma$  and  $M_{12}$  to about 1 MeV for the solutions providing  $\Gamma$  and  $M_{12}$  near the common area. Correspondingly, the resonance width increases from hundreds of eV to hundreds of keV.

#### IV. SUMMARY AND DISCUSSION

The lowest  $0^+$  states of  $^{12}\text{C}$  are calculated to study the role of the three-body interactions in the  $\alpha$ -cluster model. The method used in the present paper provides an accurate calculation of fine characteristics of  $^{12}\text{C}$ , viz., the extremely narrow width  $\Gamma$  of the  $0_2^+$  state and the  $0_2^+ \rightarrow 0_1^+$  MTME  $M_{12}$ . The two-body potentials, obtained by modification of the Ali-Bodmer potential, provide the exact energy of the  $\alpha$ - $\alpha$  resonance (the  $^8\text{Be}$  nucleus) while its width is allowed to vary within the experimental uncertainty. A simple two-Gaussian form of the three-body potential is chosen on the assumption that the potential must take into account the effects beyond the  $\alpha$ -cluster model. The experimental values of the ground- and excited-state energies and the ground-state rms radius are used to impose three restrictions on four parameters of the three-body potential. The remaining degree of freedom provides the one-parameter dependence of the width of the near-threshold  $0_2^+$  state and the  $0_2^+ \rightarrow 0_1^+$  MTME, which are experimentally available. It should be emphasized that the determination of the parameters of  $V_3(\rho)$  by fixing  $E_{gs}$ ,  $E_r$ , and  $R^{(1)}$  at the experimental values leads to rather complicated dependence of  $\Gamma$ ,  $M_{12}$ , and  $R^{(2)}$  on the  $\alpha$ - $\alpha$  interactions.

The calculations reveal that for all the two-body potentials under consideration  $\Gamma$  and  $M_{12}$  take the values about 16.5 eV and 9.0 fm<sup>2</sup> and become essentially independent of the choice of the three-body potential. At the same time, the excited-state rms radius  $R^{(2)} \approx 3.9$  fm noticeably exceeds the ground-state rms radius  $R^{(2)} = 2.47$  fm. Both  $\Gamma$  and  $M_{12}$  are well above the experimental data, which reflects a general trend for these values to be overestimated in calculations. Alternatively, for the two-body potentials corresponding to  $\gamma > 6.35$  eV, i. e., for the three-body potential with a strong attractive short-range term, both  $\Gamma$  and  $M_{12}$  decrease as the strength of the attractive term  $|V_1|$  increases and its range  $b_1$  decreases. The solutions of this kind optionally give the values of  $\Gamma$  and  $M_{12}$  which are surprisingly close to the experimental data. For these solutions, the excited-state structure undergoes a considerable modification by a strong short-range attractive potential, which entails on a considerable amplification of the short-range component of the excited-state wave function and, hence, a decrease in the rms radius to unexpectedly small values  $R^{(2)} \approx 2.8$  fm.

Against intuition, the short-range component of the ground-state wave function decreases. In addition, the attractive short-range term of the three-body potential leads to appearance of a narrow resonance above the  $0_2^+$  state.

In conclusion, a family of the effective potentials was found, which allows the experimental values for the basic characteristics of the  $^{12}\text{C}(0^+)$  states, i. e.,  $E_{gs}$ ,  $E_r$ , and  $R^{(1)}$ , to be reproduced within the framework of the  $\alpha$ -cluster model. Concerning the fine characteristics, such as  $\Gamma$ ,  $M_{12}$ , and  $R^{(2)}$ , the calculations reveal two principal choices of the effective potentials. For the first one, the calculated  $\Gamma$  and  $M_{12}$  are localized in small areas  $\Gamma \approx 16 \pm 1$  eV and  $M_{12} \approx 9 \pm 0.5$  fm<sup>2</sup>, noticeably above the experimental data. In other words, if the size of the ground state is fixed, it imposes a stringent constraint on the finer properties, i.e.,  $\Gamma$  and  $M_{12}$  for quite arbitrary potentials. For the second one, with strong short-range attraction supporting an additional narrow resonance, both  $\Gamma$  and  $M_{12}$  take a wide range of values which might be chosen near the experimental data. These solutions exist if a narrow resonance is allowed, however, there are no experimental indications of a narrow resonance above the  $0_2^+$  state. Qualitative conclusion is that if  $E_{gs}$ ,  $E_r$ , and  $R^{(1)}$  are fixed at the experimental values, a considerable short-range component of the wave function is needed to improve agreement with experiment for  $\Gamma$  and  $M_{12}$ . Certainly, the problem of reliable description of  $\Gamma$  and  $M_{12}$  in the  $\alpha$ -cluster model deserves a thorough investigation, e. g., by using the non-local three-body potential describing a coupling with twelve-nucleon channel at short distances.

- 
- [1] E. E. Salpeter, *Astrophys. J.* **115**, 326 (1952).
  - [2] F. Hoyle, *Astrophys. J. Suppl.* **1**, 121 (1954).
  - [3] L. V. Grigorenko, R. C. Johnson, I. G. Mukha, I. J. Thomson, and M. V. Zhukov, *Phys. Rev. C* **64**, 054002 (2001).
  - [4] L. V. Grigorenko and M. V. Zhukov, *Phys. Rev. C* **68**, 054005 (2003).
  - [5] H. O. U. Fynbo, Y. Prezado, U. C. Bergmann, M. J. G. Borge, P. Dendooven, W. X. Huang, J. Huikari, H. Jeppesen, P. Jones, B. Jonson, et al., *Phys. Rev. Lett* **91**, 082502 (2003).
  - [6] O. I. Kartavtsev, *Few-Body Systems* **34**, 39 (2004).
  - [7] D. N. F. Dunbar, R. E. Pixley, W. A. Wenzel, and W. Whaling, *Phys. Rev.* **92**, 649 (1953).

- [8] C. W. Cook, W. A. Fowler, C. C. Lauritsen, and T. Lauritsen, *Phys. Rev.* **107**, 508 (1957).
- [9] M. Freer, A. H. Wuosmaa, R. R. Betts, D. J. Henderson, P. Wilt, R. W. Zurmühle, D. P. Balamuth, S. Barrow, D. Benton, Q. Li, et al., *Phys. Rev. C* **49**, R1751 (1994).
- [10] A. G. W. Cameron, *Astrophys. J.* **130**, 916 (1959).
- [11] K. Nomoto, F.-K. Thielemann, and S. Miyaji, *Astron. Astrophys.* **149**, 239 (1985).
- [12] K. Langanke, M. Wiescher, and F.-K. Thielemann, *Z. Phys. A* **324**, 147 (1986).
- [13] I. Fushiki and D. Q. Lamb, *Astrophys. J.* **317**, 3621 (1987).
- [14] S. Schramm, *Astrophys. J.* **397**, 579 (1992).
- [15] Y. Funaki, A. Tohsaki, H. Horiuchi, P. Schuck, and G. Röpke, *Eur. Phys. J. A* **24**, 368 (2005).
- [16] S. I. Fedotov, O. I. Kartavtsev, V. I. Kochkin, and A. V. Malykh, *Phys. Rev. C* **70**, 014006 (2004).
- [17] D. V. Fedorov and A. S. Jensen, *Phys. Lett. B* **389**, 631 (1996).
- [18] N. N. Filikhin, *Yad. Fiz.* **63**, 1612 (2000).
- [19] S. Ali and A. R. Bodmer, *Nucl. Phys.* **80**, 99 (1966).
- [20] J. H. Macek, *J. Phys. B* **1**, 831 (1968).
- [21] F. Ajzenberg-Selove, *Nucl. Phys. A* **490**, 1 (1988).
- [22] F. Ajzenberg-Selove, *Nucl. Phys. A* **506**, 1 (1990).
- [23] W. Ruckstuhl, B. Aas, W. Beer, I. Beltrami, K. Bos, P. F. A. Goudsmit, H. J. Leisi, G. Strassner, A. Vacchi, F. W. N. D. Boer, et al., *Nucl. Phys. A* **430**, 685 (1984).
- [24] E. A. J. M. Offermann, L. S. Cardman, C. W. de Jager, H. Miska, C. de Vries, and H. de Vries, *Phys. Rev. C* **44**, 1096 (1991).
- [25] W. Reuter, G. Fricke, K. Merle, and H. Miska, *Phys. Rev. C* **26**, 806 (1982).
- [26] In the present calculation, the ground-state rms radius  $R^{(1)}$  is fixed at the elder experimental value 2.47 fm [25] that does not reflect on the conclusions.